Effects of shear layer growth on the indirect noise in compound nozzles

Khaled Younes, Jean-Pierre Hickey

Department of Mechanical and Mechatronics Engineering, University of Waterloo, Waterloo, Ontario, N2L 3G1, Canada

Abstract

A one-dimensional analytical model is proposed to account for mixing and compute the indirect noise in compound nozzle flows. The model is based on the work of Morton *et al.* (*Proceedings of the Royal Society A: Mathematical, Physical and Engineering Sciences* 234 (1196), 1956, 1–23) and serves as an extension to Younes & Hickey (*Journal of Sound and Vibration* 442, 2019, 609–623). The model is valid for subsonic flows in the limit of small velocity differences. By studying various inlet Mach numbers and area ratios, a parametric study is conducted to quantify the shear layer growth at the outlet of the nozzle. It is shown that shear layer growth is maximized at the highest convective Mach number and lowest primary area ratio. The effect of the shear layer on the indirect noise is explored by computing the entropic response with and without the presence of shear. It is shown that the effect becomes pronounced at shear layer thicknesses above 50%. In general, the shear layer acts to shift the peak noise to the left of the frequency spectrum, while attenuating the noise at high frequencies. This finding provides new insight into the design of subsonic noise suppressors for multi-stream nozzle devices.

Keywords: aeroacoustics, indirect noise, confined jets, shear layer, compound nozzle

1. Introduction

The continuous demand for quieter aircrafts has spurred considerable efforts in characterizing and reducing the noise emitted from ground and in-flight gas turbines. The culmination of those efforts resulted in the well-established notion that combustion noise is of great importance. In an aeroengine, combustion noise is typically categorized as direct and indirect noise [1]. Direct noise arises due to the local density variation in the reactive flow region as a result of the unsteady heat release intrinsic to turbulent combustion. Whereas, indirect noise is generated by the acceleration of entropic, compositional, and vortical inhomogeneities from within the combustor through flow contractions, such as nozzles and

Email address: kyounes@edu.uwaterloo.ca (Khaled Younes)

blade passages. In the context of total combustion noise, indirect noise was shown to be significant, exceeding direct noise considerations under certain flow conditions [2, 3, 4].

The propagation of entropy waves through a quasi-one-dimensional nozzle was first studied by Cuadra [5] and then by Marble & Candel [6] using a compact nozzle assumption valid in the low-frequency limit. More recent work addressed this limitation using an equivalent nozzle length correction [7, 8], a piecewise-linear mean velocity profile [9, 10], and asymptotic expansions [11, 12]. Duran & Moreau [11] developed a general approach using a Magnus [13] expansion, allowing for the computation of linear transfer functions for arbitrary flow conditions and up to any frequency, for homogeneous gas mixtures. To account for noise from compositional inhomogeneities in heterogeneous flows, Magri *et al.* [14] used the compact nozzle assumption of Marble & Candel [6] to derive analytical expressions for compositional noise. Magri [12] later generalized the solution to higher frequencies. Vortical perturbations were studied theoretically in a duct [15] and experimentally through a nozzle [16].

Common to all the aforementioned scientific works is the consideration of single-stream nozzle flows. Mixer-ejector nozzles and engine test cells, however, exhaust multiple gas streams—with different velocities, temperatures, and composition—side-by-side through the nozzle. In such a multi-stream setup, also classically referred to as *compound-compressible nozzle flow*, flow inhomogeneities in each stream have an influence on the overall behavior of the nozzle and the generation of indirect noise. This problem was studied analytically by Younes & Hickey [17], who used the compound flow relations derived by Bernstein *et al.* [18] to extend the solution of Duran & Moreau [11] and show that the area occupied by each stream at the inlet and the initial Mach number significantly impact the acoustic and entropic responses of compound nozzles. In their work, Younes & Hickey [17] assumed negligible mixing between the streams. However, this may not always be the case. In real-life situations, the streams will mix to form an intermediate shear layer that grows with the nozzle length. The shear layer will act to reduce the radiated noise by reducing the velocity of the mixing streams. A quantification of this phenomenon has not been presented and is the main objective of this work.

Mixing effects were considered in an approximate manner by Tew *et al.* [19], who assessed the performance of mixer-ejector nozzles in the presence of streamwise vorticity originating from lobed mixers. Benham *et al.* [20] presented a two-dimensional model to predict shear layer growth in confined, incompressible flows. Despite its prevalence in practical applications, the effect of the shear layer on the indirect noise generated in compound nozzles remains unknown.

In this paper, we aim to present a computationally efficient, one-dimensional approach to account for mixing in compound nozzles and quantitatively determine the impact of shear layer growth on indirect noise for the first time. The paper is organized as follows: in §2, we present a mathematical model that accounts for mixing between the streams, §3 provides a wavenumber analysis, §4 discusses the results obtained, and conclusions are drawn in §5.

2. Mathematical Model

2.1. Compound flow with shear layer growth

To account for multiple streams in the nozzle exhaust, Younes & Hickey [17] follow the formulation proposed by Bernstein *et al.* [18], assuming negligible mixing, gradual area changes, and isentropic flow with no separation. In this section, we derive an analytical model accounting for mixing of single component gases in the case of a two-stream compound nozzle. The derivation is readily extended to any n number of streams. However, we choose $n = 2$ for convenience. In the presence of a shear layer and without flow separation, the geometric constraint governing a two-stream compound nozzle is given by

$$\sum_{i=1}^{2} A_i(x) + A_s(x) = A_t(x), \tag{1}$$

where A is the cross-sectional area; the subscript $()_i$ represents the *i-th* stream; $()_s$ the shear layer; and $()_t$ the total cross-sectional area of the nozzle. A schematic diagram is shown in figure 1, where it is assumed that the shear layer is located fully within $A_s(x)$. The definition of the mass flow rate, ideal gas law, and isentropic relations are introduced in their time-averaged form as follows

$$\bar{\dot{m}}_i = \bar{\rho}_i A_i \bar{u}_i, \tag{2}$$

$$\bar{p} = \bar{\rho}_i R_i \bar{T}_i, \tag{3}$$

$$\frac{p_{oi}}{\bar{p}} = \left(1 + \frac{\gamma_i - 1}{2}\bar{M}_i^2\right)^{\frac{\gamma_i}{\gamma_i - 1}} = \left(\frac{T_{oi}}{\bar{T}_i}\right)^{\frac{\gamma_i}{\gamma_i - 1}}, \tag{4}$$

where u, p, and ρ are respectively the velocity, pressure, and density; the ratio of specific heats is denoted by $\gamma = c_p/c_v$; $\bar{\dot{m}}$ is the mean mass flow rate, R is the gas constant, $\bar{T}$ is the mean flow temperature, and p_o, T_o represent the stagnation pressure and temperature conditions, respectively. If the flow in the plug region is steady and adiabatic and undergoes strictly isentropic acceleration, R, p_o, and T_o will be constant in each stream. While the consideration of isentropic flows may appear as a drastic simplification, we show in section 4 that the total pressure losses remain under 5% in most cases studied. Further, in Appendix A, we compare the results from the isentropic solver against those obtained from a conservation of momentum analysis, applied on a simplified rectangular geometry. Then, given that the isentropic relations hold, using equations (2)–(4) and the definition of the mean flow Mach number, $\bar{M} = \bar{u}/\bar{c}$ with $\bar{c}$ as the mean flow speed of sound, the first term of (1) can be rearranged as

$$\sum_{i=1}^{2} C_i \bar{\dot{m}}_i f(\bar{p}) + A_s = A_t, \tag{5}$$

with

$$C_i = p_{oi}^{\frac{1-\gamma_i}{\gamma_i}} \sqrt{T_{oi}\left(\frac{R_i}{2}\right)\left(\frac{\gamma_i - 1}{\gamma_i}\right)}, \tag{6}$$

and

$$f(\bar{p}) = \left(\frac{1}{\bar{p}}\right)^{\frac{1}{\gamma_i}} \left[1 - \left(\frac{\bar{p}}{p_{oi}}\right)^{\frac{\gamma_i - 1}{\gamma_i}}\right]^{-1/2}. \tag{7}$$

Note that in equation (5), $\bar{p}$ is only a function of the nozzle axial position and remains constant in the radial direction. This is true for negligibly small area changes through the nozzle, $dA/dx \approx 0$, i.e. for a nozzle much longer than it is wide. The change in mass flow rate in each stream can be obtained using an entrainment assumption, as was done by Benham *et al.* [20] following Morton *et al.* [21]. For incompressible flows, this follows

$$\frac{d\bar{\dot{m}}_i}{dx} = -\frac{1}{2} S_c \bar{\rho}_i \left(\bar{u}_1 - \bar{u}_2\right), \qquad \text{with} \qquad i = 1, 2 \tag{8}$$

where S_c is a constant between 0.06–0.11 for unconfined flows [22] and 0.18 for confined flows [20]. An alternative derivation taking into account compressibility effects is given in Appendix C. For moderate mean flow Mach numbers, it was shown that density changes minimally impact the flow [23]. To fully close the system of equations, the conservation of mass is written as

$$\frac{d\bar{\dot{m}}_1}{dx} + \frac{d\bar{\dot{m}}_2}{dx} + \frac{d\bar{\dot{m}}_s}{dx} = 0, \tag{9}$$

and the velocity in the shear layer is given by Papamoschou & Roshko [24]

$$\bar{u}_s = \frac{\bar{u}_1\sqrt{\bar{\rho}_1} + \bar{u}_2\sqrt{\bar{\rho}_2}}{\sqrt{\bar{\rho}_1} + \sqrt{\bar{\rho}_2}}. \tag{10}$$

Equation (10) follows directly from a turbulent shear layer analysis based on the presence and motion of large-scale coherent structures in compressible turbulent flows [24]. For a given set of initial conditions $(\gamma_1, \gamma_2, R_1, R_2, A_1^0, A_2^0, \bar{M}_1^0, \bar{M}_2^0, \bar{T}_1^0, \bar{T}_2^0)$, nozzle geometry $A_t(x)$, and inlet pressure $\bar{p}^0$, the system of equations (5)–(10) can be solved to yield the pressure, $\bar{p}(x)$, velocity, $\bar{u}_{1,2}(x)$, and shear layer growth $A_s(x)$ along the nozzle.

2.2. Governing equations

The quasi-one-dimensional Euler equations for a calorifically perfect gas are

$$\frac{\partial}{\partial t}\left(\rho A\right) + \frac{\partial}{\partial x}\left(\rho u A\right) = 0, \tag{11}$$

$$\frac{\partial}{\partial t}\left(\rho u A\right) + \frac{\partial}{\partial x}\left(\left[p + \rho u^2\right] A\right) = p\frac{dA}{dx}, \tag{12}$$

$$\frac{\partial}{\partial t}\left(\left[\frac{p}{\gamma - 1} + \frac{1}{2}\rho u^2\right] A\right) + \frac{\partial}{\partial x}\left(\left[\frac{\gamma p}{\gamma - 1} + \frac{1}{2}\rho u^2\right] u A\right) = 0. \tag{13}$$

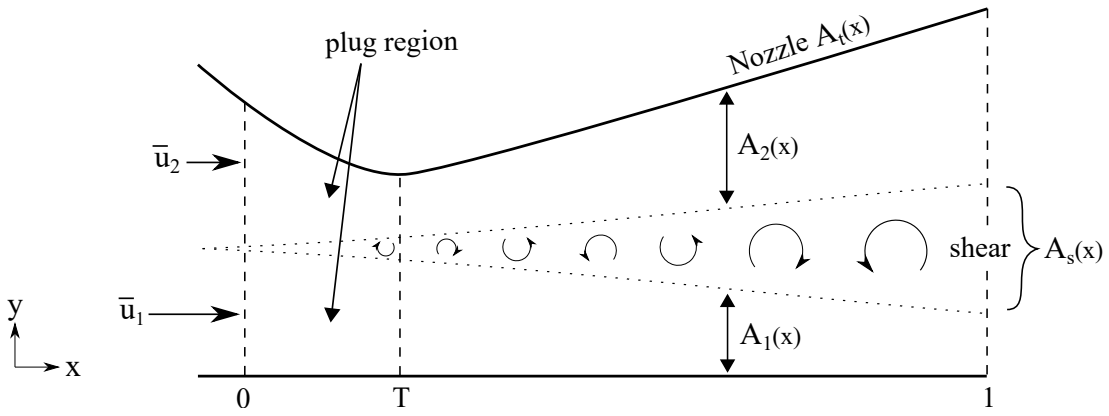

Figure 1: Diagram of an axially symmetric two-stream compound nozzle with mixing in the flow. The subscripts $()_{1,2}$ refer to the plug flow; $()_s$ the shear layer; and $()_t$ the total nozzle area.

Entropy is defined through Gibbs' relation

$$Tds = dh - \frac{dP}{\rho}, \tag{14}$$

where s, h are the entropy and enthalphy, respectively. The variables of the governing equations can be decomposed into a time-averaged mean quantity, $\bar{()}$, and a perturbation about the mean, $()'$, such that $() = \bar{()} + ()'$. Transport equations for the perturbations may be derived by neglecting the higher-order terms. The LEEs read

$$\left[\frac{\partial}{\partial t} + \bar{u}\frac{\partial}{\partial x}\right]\left(\frac{p'}{\gamma\bar{p}}\right) + \bar{u}\frac{\partial}{\partial x}\left(\frac{u'}{\bar{u}}\right) = 0, \tag{15}$$

$$\left[\frac{\partial}{\partial t} + \bar{u}\frac{\partial}{\partial x}\right]\left(\frac{u'}{\bar{u}}\right) + \frac{\bar{c}^2}{\bar{u}}\frac{\partial}{\partial x}\left(\frac{p'}{\gamma\bar{p}}\right) + \left(2\frac{u'}{\bar{u}} - (\gamma-1)\frac{p'}{\gamma\bar{p}} - \frac{s'}{c_p}\right)\frac{\partial\bar{u}}{\partial x} = 0, \tag{16}$$

$$\left[\frac{\partial}{\partial t} + \bar{u}\frac{\partial}{\partial x}\right]\left(\frac{s'}{c_p}\right) = 0, \tag{17}$$

where equation (17) is only valid for isentropic flows. For a calorifically perfect gas, the mean flow ratio of specific heats, $\bar{\gamma}$, and specific heat capacity, $\bar{c}_p$, are constants and the overbar is dropped. Equations (15)–(17) can be written in dimensionless form using: $\varepsilon = x/L$, where L is the nozzle length; $\tau = tf$, where f is a characteristic frequency of the perturbation; $\bar{M} = \bar{u}/\bar{c}$; $\psi = p'/(\gamma\bar{p})$, $\upsilon = u'/\bar{u}$, and $\sigma = s'/c_p$, where ψ, υ, σ represent the dimensionless pressure, velocity, and entropy fluctuations, respectively; and $\tilde{u} = \bar{u}/c_0$, where c_0 is the speed of sound at the inlet. The Helmholtz number, $\omega = fL/c_0$, is also introduced to relate the nozzle length with the characteristic acoustic wavelength and study non-zero frequencies.

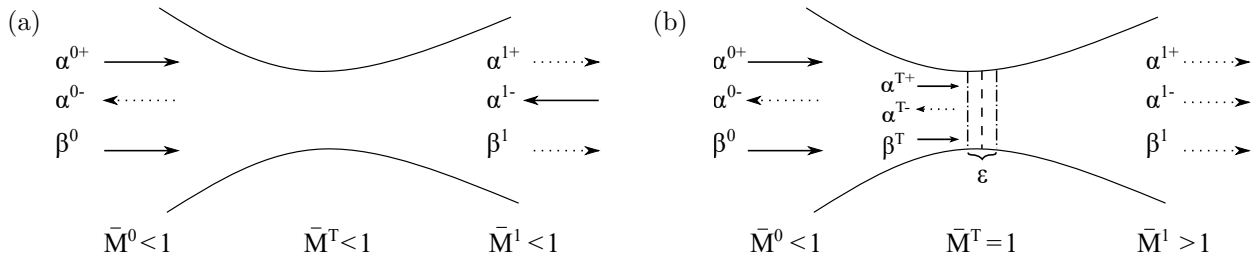

Figure 2: Downstream-propagating acoustic wave, α^+, upstream-propagating acoustic wave, α^-, and entropy wave, β, in (a) subsonic nozzle and (b) supersonic nozzle, where $()^0, ()^T, ()^1$ represent the inlet, throat, and outlet of the nozzle, respectively.

The non-dimensional LEEs are

$$\left[\omega\frac{\partial}{\partial\tau}+\tilde{u}\frac{\partial}{\partial\varepsilon}\right](\psi)+\tilde{u}\frac{\partial}{\partial\varepsilon}(\upsilon)=0, \tag{18}$$

$$\left[\omega\frac{\partial}{\partial\tau}+\tilde{u}\frac{\partial}{\partial\varepsilon}\right](\upsilon)+\frac{\bar{c}^2}{\tilde{u}}\frac{\partial}{\partial\varepsilon}(\psi)+(2\upsilon+(1-\gamma)\psi-\sigma)\frac{\partial\tilde{u}}{\partial\varepsilon}=0, \tag{19}$$

$$\left[\omega\frac{\partial}{\partial\tau}+\tilde{u}\frac{\partial}{\partial\varepsilon}\right](\sigma)=0. \tag{20}$$

Equations (18)–(20) can be solved directly by performing an asymptotic expansion in ω to u', p', and ρ' [7, 8], correcting to first-order the compact solution of Marble & Candel [6]. Alternatively, a more general solution correcting to higher-order terms can be obtained by recasting the LEEs in invariant form and performing an asymptotic expansion in ω directly to the invariants [11, 12, 17]. For brevity, a detailed solution procedure is not presented here. The interested reader is referred to [17] for more details. The boundary conditions of the invariant formulation of the generalized LEEs are given in figure 2 [11]. In terms of dimensionless fluctuations, the upstream- and downstream-propagating acoustic waves can be written as: $\alpha^{\pm}=\psi\pm\bar{M}\upsilon$ and the entropy wave as: $\beta=\sigma$.

3. Wavenumber Analysis

To compute the acoustic response of the compound nozzle, Younes & Hickey [17] recast the LEEs for each stream in invariant form and independently solve the resulting governing equations using a Magnus [13] expansion, as was done by Duran & Moreau [11]. This solution procedure assumes that the acoustic waves cannot penetrate through the infinitely-thin shear layer, i.e. the shear layer acts as a waveguide, and remains valid in the limit of high wavenumbers. However, with $A_s(x)$ now fully defined, a more precise interpretation of this assumption can be presented. In particular, the acoustic waves will reflect back onto the originating flow if the critical distance, y^*, used to define the turning level of wavepackets, lies inside the linearly sheared region [25]. Mathematically, this can be represented as

$$y^*\lesssim y_s \qquad \text{for} \qquad y^*=\pm\frac{c_0}{Sk_x}\left(\sqrt{k_x^2+k_{y0}^2}-k_x\right), \tag{21}$$

where $y_s = \sqrt{A_s/\pi}$, k_x represents the streamwise wavenumber, k_{y0} represents the initial shearwise wavenumber, and S is a shear parameter defined at the center of the sheared region to be $S = c_0 M_c/(2l + y_s)$, with l being the height of the non-linear shear region, commonly chosen to be $l \ll y_s$, and $M_c = \bar{M}_1 - \bar{M}_2$ is the convective Mach number. In the limit of high streamwise wavenumbers ($k_x \to \infty$) or infinitely-thin shear layers ($y_s \to 0$), $y^* \to 0$ and the waves reflect back for any flow condition. When $y_s \neq 0$ or the wavenumbers are finite, equation (21) can be rearranged to provide a general condition in which the waveguide assumption holds. By taking $y^* = y_s$ and solving for the wavenumber ratio, this can be written as

$$\frac{k_x}{k_{y0}} > \frac{1}{\sqrt{(M_c + 1)^2 - 1}}. \tag{22}$$

Note that there exists a discontinuity in the solution of (22) at $M_c = 0$, when the streams are identical. Thus, the solution is only valid for dissimilar streams. In the case of identical streams at $M_c = 0$, the nozzle can be considered single-stream and the perturbations are independent for any flow condition. From equation (22), it is clear that extra care must be taken in the choice of wavenumbers at small convective Mach numbers. As the convective Mach number increases, the wavenumber ratio required to satisfy the waveguide assumption drops rapidly due to the inverse proportionality relation: $k_x/k_{y0} \propto M_c^{-1}$.

4. Results

The mathematical model presented in §2 is used to solve for the indirect noise generated in each stream of a two-stream compound nozzle, accounting for mixing in the flow. Here, we formally define the indirect noise to be the response due to an entropic perturbation at the inlet, i.e. $\beta^0 = 1$. The nozzle under study is that of the NASA Converging-Diverging Verification (CDV) case [see 26, 4.11b], with an inlet section of $A_t^0/A^T = 2.5$, outlet section $A_t^1/A^T = 1.5$, and throat position $x^T = 0.5L$. This idealized nozzle geometry is selected because the area changes are gradual, no flow separation is expected, and the isentropic relations hold. We stress that a slight deviation from the isentropic relations is expected in the presence of mixing. This is quantified in Appendix A, where the maximum deviation is found to be $\approx 25\%$ at the outlet of the domain. Despite that, for small velocity differences between the streams, the isentropic relations provide accurate estimates of the flow. The initial conditions are taken to be: $\bar{T}^0_{1,2} = 298$ K and $\bar{p}^0 = 1$ atm. The two streams are assumed to be identical, with a specific heat ratio and gas constant of ambient air. The nozzle length is arbitrarily chosen as 10 unit lengths. First, the shear layer growth is quantified for a wide range of inlet Mach numbers and area ratios. This serves as a parametric study of the variables controlling the shear growth rate. Second, to assess the impacts of mixing on the indirect noise, the entropic response of the nozzle is computed up to $\omega = 0.5$ with and without the presence of a shear layer. Finally, the total pressure losses are calculated to verify the isentropicity of the flow.

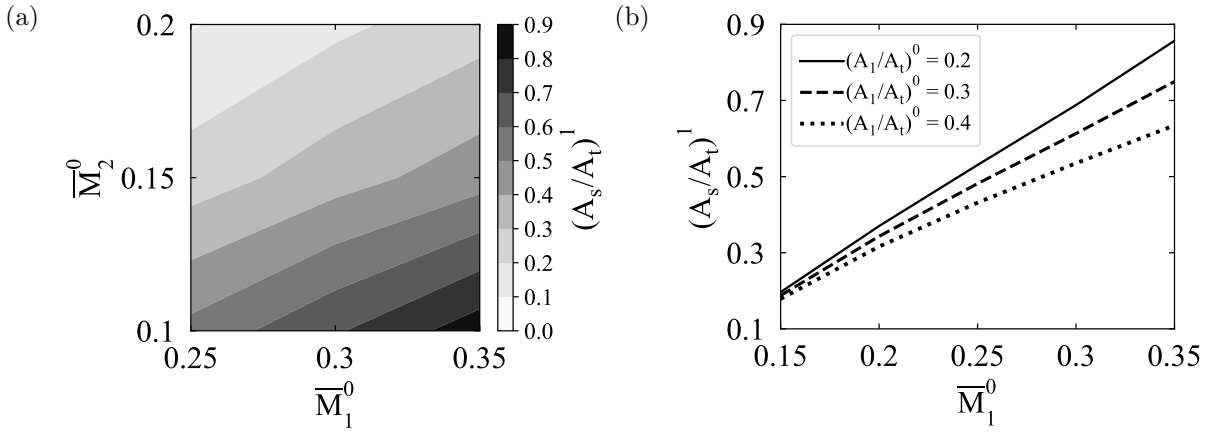

Figure 3: Shear layer growth as a function of (a) inlet Mach number for $(A_1/A_t)^0 = 0.2$ and (b) inlet area ratio for $\bar{M}_2^0 = 0.1$.

4.1. Shear layer growth

The maximum shear layer growth at the outlet is computed for a total of 21 cases using $S_c = 0.18$ for confined flows [20]. Results obtained by varying the inlet Mach number of the streams are shown in figure 3a, while results obtained by varying the inlet area ratio of the primary stream are given in figure 3b. Two main observations can be noted. First, the largest shear layer growth is obtained at the highest convective Mach number (recall that $M_c = \bar{M}_1 - \bar{M}_2$). This is expected because the change in mass flow rate is directly proportional to the velocity difference in the streams, as given by equation (8). Second, at a constant convective Mach number, lower primary area ratios yield larger growth rates. This can be attributed to the smaller mass flow rates obtained at lower area ratios. Given all other variables are held constant, shear layer growth is more pronounced at smaller flow rates.

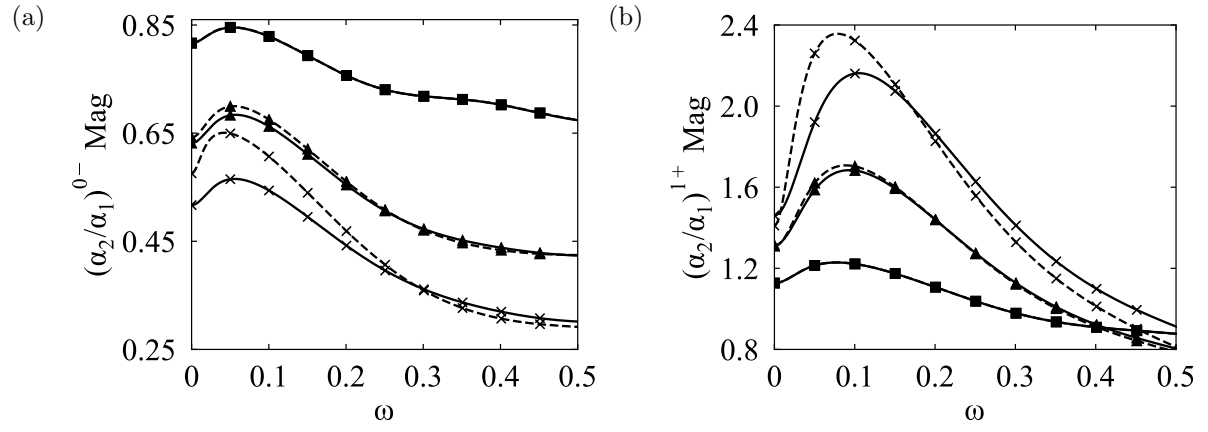

Figure 4: Magnitude of the indirect noise ratio at the (a) inlet and (b) outlet for $(A_1/A_t)^0 = 0.2$ and $\bar{M}_2^0 = 0.1$. Solid lines ($-$) show results obtained without a shear layer, while dashed lines ($--$) include a shear layer in the analysis. (■): $\bar{M}_1^0 = 0.15$; (▲): $\bar{M}_1^0 = 0.25$; (×): $\bar{M}_1^0 = 0.35$.

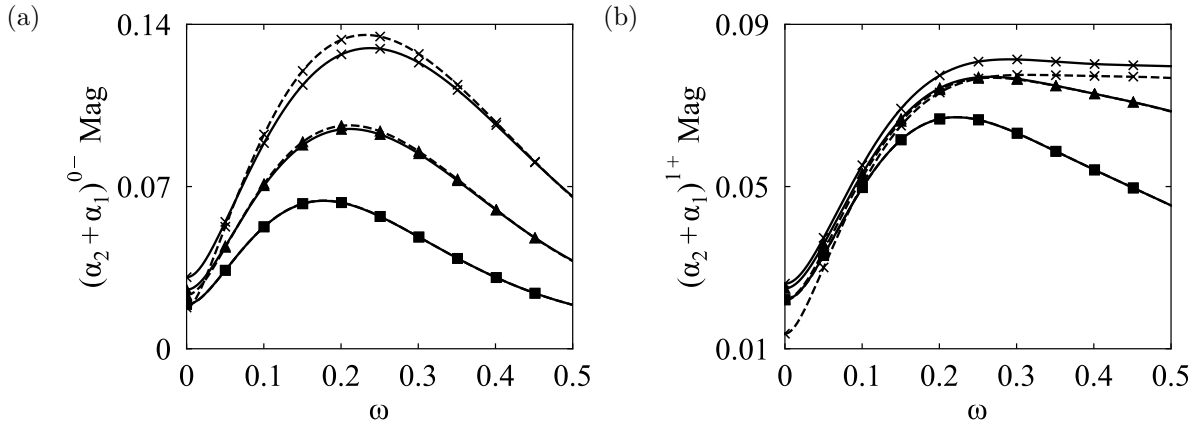

Figure 5: Total indirect noise at the (a) inlet and (b) outlet for $(A_1/A_t)^0 = 0.2$ and $\bar{M}_2^0 = 0.1$. Solid lines $(-)$ show results obtained without a shear layer, while dashed lines $(--)$ include a shear layer in the analysis. (■): $\bar{M}_1^0 = 0.15$; (▲): $\bar{M}_1^0 = 0.25$; (×): $\bar{M}_1^0 = 0.35$.. (■): $\bar{M}_1^0 = 0.15$; (▲): $\bar{M}_1^0 = 0.25$; (×): $\bar{M}_1^0 = 0.35$.

4.2. Indirect noise with shear

The impact of the shear layer on the compound flow is quantified by first plotting the ratio of indirect noise of the slow secondary stream to the fast primary stream, α_2/α_1 (figure 4). Second, the overall indirect noise contribution from both streams, $\alpha_2 + \alpha_1$, is plotted in figure 5. Third, the phase difference between the streams, $\alpha_2 - \alpha_1$, is plotted in figure 6. Here, the primary area ratio at the inlet is $(A_1/A_t)^0 = 0.2$ and the secondary stream Mach number is held constant at $\bar{M}_2^0 = 0.1$. The corresponding Mach number distribution in the nozzle is shown in figure 7. A fifth-order Magnus [13] series is chosen for the asymptotic expansion. A grid-refinement study is conducted and a grid-independent solution with 2500 equal subdivisions is verified (result not shown). The waveguide assumption is considered valid and the wavenumber selection is done according to (22).

Figure 4a shows the magnitude of the reflected acoustic wave. This wave may create a positive feedback loop that results in thermoacoustic instabilities in combustion chambers and rocket engines [27]. For all cases studied, the reflected acoustic waves produced by the primary stream (stream 1) are greater than the slow secondary stream (stream 2), evidenced by the ratio $(\alpha_2/\alpha_1)^{0-} < 1$. This can be linked to the higher mean flow Mach number of the primary stream at the inlet. For moderate changes in mean flow properties, it can be shown that the low-frequency acoustic response at the inlet due to an entropic excitation depends mainly on $M^0(M^1 - M^0)/(1 - M^0)$ [6]. Thus, larger inlet Mach numbers result in more amplified upstream-propagating waves. A similar observation was noted by Younes & Hickey [17]. The waves of both streams are approximately equal for the lowest convective Mach number case due to the relatively small degree of asymmetry in the nozzle; $M_c \approx 0$ for $\bar{M}_1^0 = 0.15$ and $\bar{M}_2^0 = 0.1$. Additionally, the responses monotonically decrease at higher frequencies.

The magnitude of the downstream-propagating acoustic waves is presented in figure 4b. These waves are radiated to the atmosphere and are hence directly responsible for noise

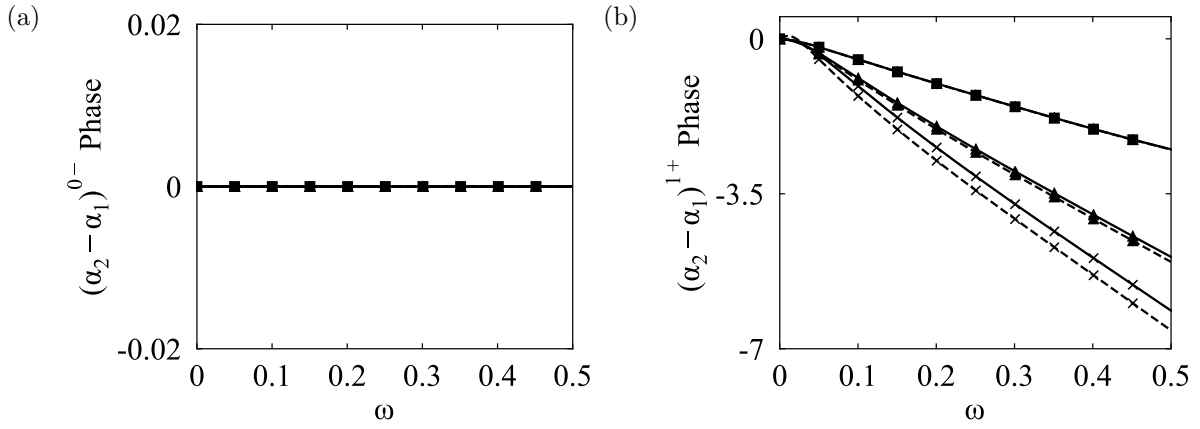

Figure 6: Phase difference of the acoustic waves at the (a) inlet and (b) outlet for $(A_1/A_t)^0 = 0.2$ and $\bar{M}_2^0 = 0.1$. Solid lines $(-)$ show results obtained without a shear layer, while dashed lines $(--)$ include a shear layer in the analysis. (■): $\bar{M}_1^0 = 0.15$; (▲): $\bar{M}_1^0 = 0.25$; (×): $\bar{M}_1^0 = 0.35$.

pollution. Due to the dipole nature of entropy noise, here, the waves produced by the slow secondary stream exceed those produced by the fast primary stream, evidenced by the ratio $(\alpha_2/\alpha_1)^{1+} > 1$. This is because the slow stream experiences stronger variations in mean flow properties, which, in turn, creates more indirect noise [6]. At the outlet, the magnitude of the acoustic transfer function is proportional to $M^1(M^1 - M^0)/(1 + M^1)$. As the evolution of the flow field determines M^1, variations in mean flow properties greatly influence the indirect noise generation. Similar to figure 4a, the responses approach unity at the lowest convective Mach number and decay at higher frequencies, although nonlinearly. Physically, it can be inferred that the energy loss through the outlet boundary increases with frequency.

From figures 4 and 5, some comments can be made on the effects of shear layer growth on indirect noise. For shear growth rates $(A_s/A_t)^1 > 50\%$, the mixing layer analyses (dashed lines) begin to diverge from the equivalent cases assuming negligible mixing (solid lines). This shows that the shear layer plays an increasingly important role at high convective Mach numbers or small flow rates and cannot be neglected. The presence of the shear layer appears to shift the indirect noise peak to the left, towards lower frequencies. Moreover, it dampens the high-frequency noise at a faster rate in comparison to the cases without a shear layer. These changes to the noise indicate that the shear layer affects the evolution of the Mach number over the entire nozzle length and not just the outlet value, a statement confirmed by figure 7a, where stronger deceleration is present as a result of mixing. Physically, this implies that mixing can be utilized as a means of altering the noise signature of a given compound nozzle. Indeed, this was the main premise behind the design and operation of mixer-ejector nozzles in the early 90's [28]. Finally, looking at figure 6, we can deduce that the shear layer only impacts the phase of the waves at the outlet. This is expected because the phase depends solely on the boundary values of the Mach number [17]. The upstream- and downstream-propagating acoustic waves travel at the speed of sound relative to the mean flow, $\bar{u} - \bar{c}$ and $\bar{u} + \bar{c}$, respectively. Since the inlet Mach number is constant in the cases studied with or without a shear, no phase difference is seen in figure 6a. However,

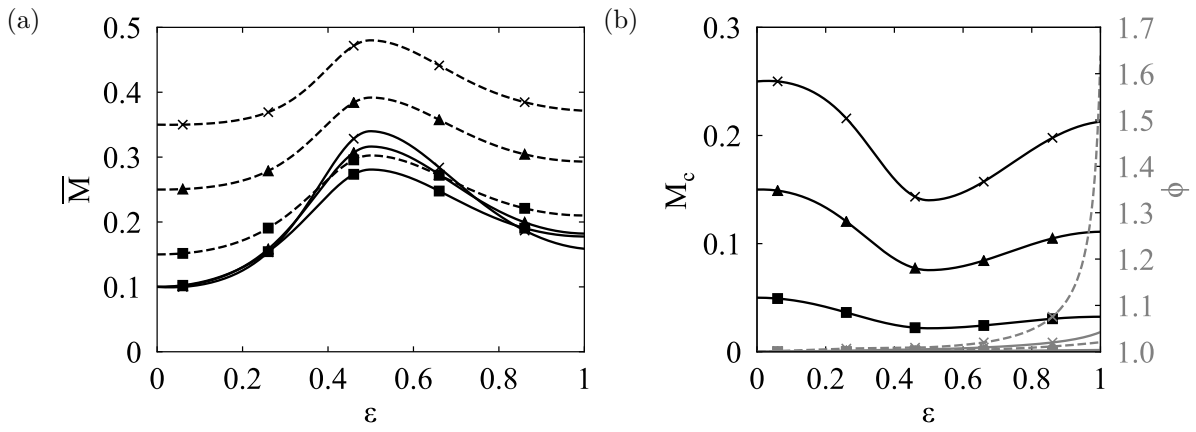

Figure 7: Evolution of the (a) Mach number and (b) convective Mach number along the nozzle length. Solid lines (−) show the secondary stream, while dashed lines (−−) represent the primary stream. Gray lines show the total pressure losses, $\phi = p_o^0/p_o^1$. (■): $\bar{M}_1^0 = 0.15$; (▲): $\bar{M}_1^0 = 0.25$; (×): $\bar{M}_1^0 = 0.35$.

the outlet Mach number is dependent on the shear layer growth. Particularly, lower outlet Mach numbers are obtained at higher growth rates. This translates to a longer time lag and a larger (more negative) phase (figure 6b). The linear phase behavior of the plots indicates that the nozzle length is acting as a linear phase shifter.

The analysis presented in this section opens up new possibilities in acoustic response mitigation of subsonic confined flows. One possibility, for example, involves a carefully designed compound nozzle that shifts the low-frequency noise peak to lie within a desired range while quieting down the higher frequencies.

4.2.1. Comments on noise considerations

The developed framework is intended to provide rapid estimates on the acoustic responses and indirect noise of plug flows in compound nozzles. To this end, the hydrodynamic noise created within the mixing layer is not accounted for. The tremendous complexities associated with turbulence-generated noise often render simple analytical tools such as ours as largely incompatible. We do not attempt to capture this mechanism of direct noise generation as it is not the focus of this work. Two points constrain the applicability of our model and should be stressed: (1) the acoustic-vortex dissipation in the shear layer, and (2) the isentropic assumption implicit in the development.

First, in general, ambient turbulent flows act to attenuate acoustic waves through scattering and absorption [29]. Given the planar nature of the waves investigated in our work, which propagate essentially parallel to the shear layer, only absorption is examined. That said, the experimental findings of Peters *et al.* [30] shed light on the fact that a quasi-laminar theory can be used to approximate the viscous damping of turbulent flows at sufficiently high frequencies, or, in the limit of $\delta_{ac} \ll \delta_l$. Here, δ_{ac} is the acoustic shear layer thickness, $\delta_{ac} = \sqrt{2\nu/f}$ with ν as the kinematic viscosity, and δ_l is the thickness of the viscous sublayer in wall-bounded flows. We assume δ_l to be related to the shear layer thickness in our case. In the quasi-laminar approach, the propagation of the acoustic waves is solely governed by

mean flow convection and turbulent stresses have no impact on the acoustic damping [31]. Thus, this imposes a limit on the Helmholtz numbers that can be studied. Particularly, the following condition must be satisfied: $\omega \gg 2\pi\nu L/A_s c_0$. Given that $\nu L \ll A_s c_0$, this condition is generally met. Caution should be taken when the shear layer is small; this will limit the validity of the quasi-laminar theory to strictly very high frequencies.

Second, indirect noise estimates are only valid when the mixing process does not yield large entropy production. While the presence of a shear layer, which is inherently unstable, between the streams should theoretically invalidate the isentropic assumption, we show in Appendix A that the isentropic relations are within 25% of the solution obtained from the conservation equations. In addition, in Appendix B, we derive a model for entropy production in each stream, similar to the formulation proposed by Papamoschou [23], and verify our constant total pressure assumption. We demonstrate that the total pressure loss, ϕ, scales with M_c^2/A (Appendix B). The losses are plotted schematically in figure 7b for all the cases studied. As can be seen, the losses become significant only for the primary stream ($\phi_1 > 30\%$) at $\varepsilon > 0.98$ and $\bar{M}_1^0 = 0.35$. This corresponds to the limiting case. In all other cases, the losses do not exceed 5% for either stream and can be neglected. Overall, since there is moderate deviation from isentropy, as a first-order estimate, the flow can be assumed isentropic.

5. Conclusions

In compound multi-stream nozzles, differential velocity differences drive the streams to mix and result in the formation of intermediate shear layers. In this paper, a simple one-dimensional analytical model is presented to account for those mixing effects and quantify their impact on indirect noise in the subsonic regime. The model uses an entrainment analogy derived by Morton *et al.* [21] to compute the shear layer growth and an asymptotic expansion to solve for the indirect noise in the plug region. The model hinges on two fundamental assumptions: namely, fully attached isentropic flow and the absence of mean radial pressure differences. These assumptions hold at low convective Mach numbers and for small total area changes. A parametric study is conducted on an idealized, two-stream nozzle geometry exploring the variables that control the shear layer growth. The convective Mach number and area ratio at the inlet are varied in a wide range. Maximum shear layer growth was obtained at the highest convective Mach number and lowest primary area ratio, corresponding to the smallest mass flow rate. Indirect noise was computed for a selected number of cases in the presence of a shear layer and by neglecting mixing in the nozzle. It was shown that the presence of a shear layer is significant and cannot be neglected for shear thicknesses above 50%. Additionally, the shear layer influences the resulting transfer functions in two main ways. First, it acts to shift the indirect noise peak towards lower frequencies. Second, it dampens the high-frequency noise faster than the cases with no shear. These results provide more insight into the acoustic response of multi-stream devices and are relevant in the design of new generation subsonic mixer-ejector nozzles and engine test cells. Finally, a wavenumber analysis is presented. This formalizes the waveguide assumption of Younes & Hickey [17] and provides a generic condition where the assumption

holds.

Acknowledgements

Fruitful discussions with Dr. Graham P. Benham are acknowledged.

Appendix A. Conservation of Momentum Analysis

The conservation of mass, momentum, and energy equations write

$$\frac{d}{dx}\left(\int_0^{A_t} \dot{m}\ dy\right) = 0, \tag{A.1}$$

$$\frac{d}{dx}\left(\int_0^{A_t} \rho u^2 dy\right) + \frac{d}{dx}\left(pA_t\right) = \tau_s, \tag{A.2}$$

$$\frac{d}{dx}\left(\int_0^{A_t} \dot{m}(c_pT + 0.5u^2) dy\right) = 0, \tag{A.3}$$

where the time-averaged overbar is dropped for brevity. In (A.2), $\tau_s = \tau_{max} = -c_\tau \rho(\Delta u)^2$, with $c_\tau = 0.013$ from the experiments of Wygnanski and Fiedler [32], represents the losses associated with shear layer growth; it is derived in more detail in Appendix B. The conservation equations are solved for a rectangular geometry having an area $A_t(x) = A_t^0/A^T = 2.5$ (equal to the inlet area of the nozzle in §4) and for conditions replicating the maximum shear layer growth at the outlet ($M_1^0 = 0.35, M_2^0 = 0.1, A_1^0/A_t^0 = 0.2$). The assumptions taken are identical to those presented in §2.1, minus the isentropic flow assumption.

The Mach number evolution is shown in figure A.8a for both solvers; the deviation is plotted in figure A.8b. As can be seen, the deviation remains under 20% for $\varepsilon < 0.8$. Since this represents a severely limiting case, where the shear layer growth is maximized at the outlet, the use of the isentropic relations is deemed appropriate for the proposed low-order model.

Appendix B. Model for Entropy Production

We recall the conservation equations for the time-averaged mass, momentum, and energy. We assume that there exists a dividing streamline where no mass transfer exists, similar to the assumption in [23], and write the equations in a slightly modified form

$$\frac{d\bar{\rho}_i}{\bar{\rho}_i} + \frac{d\bar{u}_i}{\bar{u}_i} + \frac{dA_i}{A_i} = 0, \tag{B.1}$$

$$\bar{u}_i \frac{d\bar{u}_i}{dx} + \frac{1}{\bar{\rho}_i}\frac{dp}{dx} = \frac{\tau}{\bar{\rho}_i A_i}, \tag{B.2}$$

$$\frac{dH_i}{dx} = \frac{q}{\bar{\rho}_i \bar{u}_i A_i}. \tag{B.3}$$

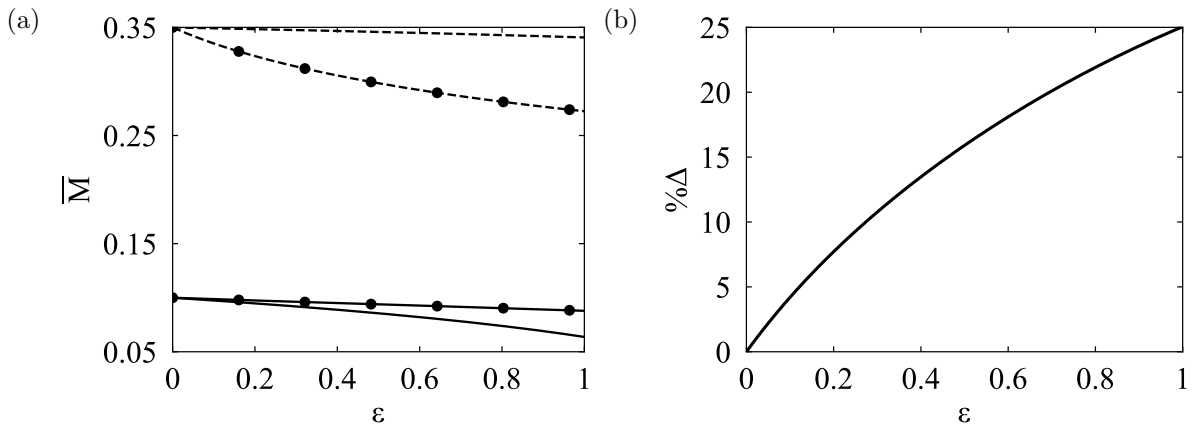

Figure A.8: (a) Evolution of the Mach number for the isentropic solver (no marker) and conservative solver (•). Solid lines (−) show the secondary stream, while dashed lines (−−) represent the primary stream. (b) Deviation in flow properties plotted as a function of the spatial coordinate.

In the above, τ is the shear stress, H_i is the total enthalpy of stream i, and q is the heat transfer to the stream (from the other stream). As done in the main text, we only consider the viscous losses in the shear layer (and not at the wall) and assume that the physical walls of the system are adiabatic. The change in entropy in a given stream is well-known

$$ds_i = \frac{1}{\bar{T}_i}\left(dh_i - \frac{dp}{\bar{\rho}_i}\right). \tag{B.4}$$

Defining the entropy flux as $\dot{s}_i = \dot{\bar{m}}_i \Delta s_i = \bar{\rho}_i \bar{u}_i A_i \Delta s_i$ and using the conservation equations (B.1)–(B.3), the change in entropy flux can be written as

$$\frac{d\dot{s}_i}{dx} = \frac{1}{\bar{T}_i}\left[q - \bar{u}_i \tau\right]. \tag{B.5}$$

Assuming negligible heat transfer ($q \approx 0$, adiabatic flow), the entropy generation is then

$$\frac{d\dot{s}_i}{dx} = -\frac{\bar{u}_i \tau}{\bar{T}_i}. \tag{B.6}$$

Following Brown & Roshko [33], the maximum shear stress can be related to

$$\tau_{max} \propto \frac{dA_s}{dx} \bar{\rho}_{avg} \bar{u}_{avg} \Delta\bar{u}, \tag{B.7}$$

where $\bar{\rho}_{avg} = \bar{\rho}_1 = \bar{\rho}_2 = \bar{\rho}$ (incompressible flow), $\bar{u}_{avg} = (\bar{u}_2 + \bar{u}_1)/2$, and $\Delta\bar{u} = \bar{u}_2 - \bar{u}_1$. Then, the shear layer growth rate dA_s/dx is proportional to $\Delta\bar{u}/\bar{u}_{avg}$ [23] and we can rewrite the maximum shear stress as

$$\tau_{max} \propto \bar{\rho}(\Delta\bar{u})^2. \tag{B.8}$$

For subsonic streams, we can write (B.8) as an equality

$$\tau_{max} = c_\tau \bar{\rho}(\Delta\bar{u})^2, \tag{B.9}$$

The entropy flux in a single stream becomes

$$\frac{d\dot{s}_i}{dx} = -0.013\frac{\bar{\rho}\bar{u}_i(\Delta\bar{u})^2}{\bar{T}}, \tag{B.10}$$

and the change in total pressure between the inlet and outlet of the nozzle can be related to the entropy change (we drop the subscript to identify the stream for clarity) using

$$-R\ln\left(\frac{p_o^0}{p_o^1}\right) = \Delta s, \tag{B.11}$$

$$\phi = \frac{p_o^0}{p_o^1} = \exp\left(\frac{-\dot{s}}{\bar{\dot{m}}R}\right). \tag{B.12}$$

Finally, by taking the spatial derivative of (B.12), we obtain

$$\frac{1}{\phi}\frac{d\phi}{dx} = \frac{-1}{\bar{\dot{m}}R}\frac{d\dot{s}}{dx}, \tag{B.13}$$

$$\frac{1}{\phi}\frac{d\phi}{dx} = \frac{0.013(\Delta\bar{u})^2}{AR\bar{T}} = \frac{0.013\gamma M_c^2}{A}. \tag{B.14}$$

Assuming that the area remains finite

$$\therefore \frac{1}{\phi}\frac{d\phi}{dx} \propto \frac{M_c^2}{A}. \tag{B.15}$$

Appendix C. Compressibility Derivation

The change in mean mass flow rate for stream 1 in the plug region written in full is

$$\frac{d\bar{\dot{m}}_1}{dx} = \frac{d\bar{\rho}_1}{dx}A_1\bar{u}_1 + \bar{\rho}_1\frac{dA_1\bar{u}_1}{dx}. \tag{C.1}$$

Under the incompressible flow assumption, the first term on the right-hand side vanishes and equation (8) is recovered. Without loss of generality, using the ideal gas law (3) and isentropic relation (4), the density can be written as

$$\bar{\rho}_1 = K_1 \left(\bar{p}\right)^{\frac{1}{\gamma_1}} \qquad \text{with} \qquad K_1 = \left(R_1 T_{o1}\right)^{-1} \left(p_{o1}\right)^{\frac{\gamma_1 - 1}{\gamma_1}} . \tag{C.2}$$

Taking the derivative of (C.2) with respect to x yields

$$\frac{d\bar{\rho}_1}{dx} = \frac{\bar{\rho}_1}{\gamma_1 \bar{p}} \frac{d\bar{p}}{dx}. \tag{C.3}$$

By substituting (C.3) in (C.1), we get

$$\frac{d\bar{\dot{m}}_1}{dx} = \frac{\bar{\dot{m}}_1}{\gamma_1 \bar{p}} \frac{d\bar{p}}{dx} - \frac{1}{2} S_c \bar{\rho}_1 \left(\bar{u}_1 - \bar{u}_2\right), \tag{C.4}$$

which is an alternative differential equation that can be solved in place of (8) to take into account streamwise density changes. A similar equation could be written for stream 2 by replacing the subscript $()_1$ with $()_2$. Since no new variables are introduced, the system of equations remains closed and can be solved.

References

[1] W. C. Strahle, "Some results in combustion generated noise," *Journal of Sound and Vibration*, vol. 23, no. 1, pp. 113–125, 1972.

[2] S. Candel, *Analytical Studies of Some Acoustic Problems of Jet Engines*. PhD thesis, California Institute of Technology, 1972.

[3] M. Leyko, F. Nicoud, and T. Poinsot, "Comparison of Direct and Indirect Combustion Noise Mechanisms in a Model Combustor," *AIAA Journal*, vol. 47, no. 11, pp. 2709–2716, 2009.

[4] M. S. Howe, "Indirect combustion noise," *Journal of Fluid Mechanics*, vol. 659, pp. 267–288, 2010.

[5] E. Cuadra, "Acoustic Wave Generation by Entropy Discontinuities Flowing Past an Area Change," *The Journal of the Acoustical Society of America*, vol. 42, no. 4, pp. 725–732, 1967.

[6] F. E. Marble and S. M. Candel, "Acoustic disturbance from gas non-uniformities convected through a nozzle," *Journal of Sound and Vibration*, vol. 55, no. 2, pp. 225–243, 1977.

[7] S. R. Stow, A. P. Dowling, and T. P. Hynes, "Reflection of circumferential modes in a choked nozzle," *Journal of Fluid Mechanics*, vol. 467, pp. 215–239, 2002.

[8] C. S. Goh and A. S. Morgans, "Phase prediction of the response of choked nozzles to entropy and acoustic disturbances," *Journal of Sound and Vibration*, vol. 330, no. 21, pp. 5184–5198, 2011.

[9] W. H. Moase, M. J. Brear, and C. Manzie, "The forced response of choked nozzles and supersonic diffusers," *Journal of Fluid Mechanics*, vol. 585, pp. 281–304, 2007.

[10] A. Giauque, M. Huet, and F. Clero, "Analytical Analysis of Indirect Combustion Noise in Subcritical Nozzles," *Journal of Engineering for Gas Turbines and Power*, vol. 134, no. 11, pp. 111–202, 2012.

[11] I. Duran and S. Moreau, "Solution of the quasi-one-dimensional linearized Euler equations using flow invariants and the Magnus expansion," *Journal of Fluid Mechanics*, vol. 723, pp. 190–231, 2013.

[12] L. Magri, "On indirect noise in multicomponent nozzle flows," *Journal of Fluid Mechanics*, vol. 828, no. R2, pp. 1–13, 2017.

[13] W. Magnus, "On the exponential solution of differential equations for a linear operator," *Communications on Pure and Applied Mathematics*, vol. 7, no. 4, pp. 649–673, 1954.
[14] L. Magri, J. O'Brien, and M. Ihme, "Compositional inhomogeneities as a source of indirect combustion noise," *Journal of Fluid Mechanics*, vol. 799, no. R4, pp. 1–12, 2016.
[15] M. S. Howe and J. T. C. Liu, "The generation of sound by vorticity waves in swirling duct flows," *Journal of Fluid Mechanics*, vol. 81, no. 2, pp. 369–383, 1977.
[16] N. Kings and F. Bake, "Indirect combustion noise: noise generation by accelerated vorticity in a nozzle flow," *International journal of spray and combustion dynamics*, vol. 2, no. 3, pp. 253–266, 2010.
[17] K. Younes and J.-P. Hickey, "Indirect noise prediction in compound, multi-stream nozzle flows," *Journal of Sound and Vibration*, vol. 442, pp. 609–623, 2019.
[18] A. Bernstein, W. H. Heiser, and C. Hevenor, "Compound-Compressible Nozzle Flow," *ASME Journal of Applied Mechanics*, vol. 34, no. 3, pp. 548–554, 1967.
[19] D. E. Tew, B. S. Teeple, and I. A. Waitz, "Mixer-Ejector Noise-Suppressor Model," *Journal of Propulsion and Power*, vol. 14, no. 6, pp. 941–950, 1998.
[20] G. P. Benham, A. A. Castrejon-Pita, I. J. Hewitt, C. P. Please, R. W. Style, and P. A. D. Bird, "Turbulent shear layers in confining channels," *Journal of Turbulence*, vol. 19, no. 6, pp. 431–445, 2018.
[21] B. R. Morton, G. Taylor, and J. S. Turner, "Turbulent Gravitational Convection from Maintained and Instantaneous Sources," *Proceedings of the Royal Society A: Mathematical, Physical and Engineering Sciences*, vol. 234, no. 1196, pp. 1–23, 1956.
[22] S. B. Pope, *Turbulent Flows*. Cambridge: Cambridge University Press, 2000.
[23] D. Papamoschou, "Model for Entropy Production and Pressure Variation in Confined Turbulent Mixing," *AIAA Journal*, vol. 31, no. 9, pp. 1643–1650, 1993.
[24] D. Papamoschou and A. Roshko, "The compressible turbulent shear layer: An experimental study," *Journal of Fluid Mechanics*, vol. 197, pp. 453–477, 1988.
[25] J.-N. Hau and B. Müller, "Acoustic wave propagation in a temporal evolving shear-layer for low-Mach number perturbations," *Physics of Fluids*, vol. 30, no. 016105, pp. 1–14, 2018.
[26] M.-S. Liou, "A generalized procedure for constructing an upwind based TVD scheme," in *25th AIAA Aerospace Sciences Meeting*, (Reno, NV, USA), 1987.
[27] L. Crocco, "Research on combustion instability in liquid propellant rockets," in *Proceedings of the 12th International Symposium on Combustion*, pp. 85–99, The Combustion Institute, 1969.
[28] W. Lord, C. Jones, A. Stern, V. Head, and E. Krejsa, "Mixer-ejector nozzle for jet noise suppression," in *26th Joint Propulsion Conference*, (Orlando, FL, USA), 1990.
[29] M. S. Howe, "The damping of sound by wall turbulent shear layers," *The Journal of the Acoustical Society of America*, vol. 98, no. 3, pp. 1723–1730, 1995.
[30] M. C. A. M. Peters, A. Hirschberg, A. J. Reijnen, and A. P. J. Wijnands, "Damping and reflection coefficient measurements for an open pipe at low Mach and low Helmholtz numbers," *Journal of Fluid Mechanics*, vol. 256, pp. 499–534, 1993.
[31] D. Ronneberger and C. D. Ahrens, "Wall shear stress caused by small amplitude perturbations of turbulent boundary-layer flow: an experimental investigation," *Journal of Fluid Mechanics*, vol. 83, no. 3, pp. 433–464, 1977.
[32] L. Wygnanski and H. E. Fiedler, "The Two-Dimensional Mixing Region," *Journal of Fluid Mechanics*, vol. 41, pp. 327–361, 1970.
[33] G. L. Brown and A. Roshko, "On density effects and large structure in turbulent mixing layers," *Journal of Fluid Mechanics*, vol. 64, no. 4, pp. 775–816, 1974.